# Essential Fracture Work of Nylon 6-Silicate Nanocomposites

**Y. Qiao, S. Avlar, S. S. Chakravarthula**

*Department of Civil Engineering, University of Akron, Akron, Ohio*

Received 21 January 2004; accepted 23 July 2004
DOI 10.1002/app.21241
Published online in Wiley InterScience (www.interscience.wiley.com).

**ABSTRACT:** In a fracture experiment of polymers, the total fracture work usually consists of an essential part associated with the plastic deformation at the crack tip and a nonessential part related to the viscous relaxation in the background. In this article, the essential fracture work in nylon 6-silicate nanocomposites is measured through a series of double-notched-sample (DNS) tests. The samples are of different silicate contents and crystallization conditions. As the cooling rate rises, the essential work is nearly constant while the total fracture work increases considerably, which should be attributed to the change in effective viscosity. © 2004 Wiley Periodicals, Inc. J Appl Polym Sci 95: 815–819, 2005

**Key words:** fracture; nanocomposites; nylon; essential work; cooling rate

## INTRODUCTION

The superior properties of nylon 6-silicate nanocomposites such as high stiffness and strength, low permeability, and high combustion resistance, make them attractive for a variety of engineering applications.[1–3] However, usually as a "side effect," the addition of the silicate nanofillers will increase the level of brittleness by suppressing plastic deformation at the crack tip, which greatly limits the application of these materials in load-bearing structures.[4–6]

In a recent experimental study,[7] this embrittlement effect was confirmed in fracture tests of air cooled nylon 6-silicate nanocomposites. As the silicate content increased from 0 to 3.7 wt %, the fracture work, $W_f$, was reduced by a factor around 5. However, in the fracture experiments of cold water quenched samples, it was found that the values of $W_f$ were at the same level regardless of the silicate content change, that is, increasing cooling rate has a beneficial effect to the fracture resistance. This phenomenon provides a promising way for the simultaneous enhancement of tensile modulus, strength, and toughness, while the associated mechanisms are still inadequately understood. With increasing of the cooling rate, the characteristic time of crystallization is reduced and as a result the nonisothermal nature must be taken into consideration.[8,9] This, together with the effect of heterogeneous nucleation at the silicate-matrix interface, leads to the fine semicrystalline structure and relatively high tie-molecule density.[10] On the other hand, with a high silicate content crazing is dominant, which is constrained by the nanofillers due to the difficulty in initiation and growth.[11,12] Increase in cooling rate also tends to promote $\gamma$ crystal form, while the contribution of the $\alpha$ crystal form can still be significant.[13] These effects further increase the complexity of the plastic deformation process.

Usually, in fracture experiments of nylon polymers at room temperature, the measured total fracture work consists of two parts: essential work and nonessential work. The former is related to cold drawing, crazing, and/or shear banding at the crack tip, which actually governs the crack growth; and the latter is caused by the viscous relaxation in the background, as depicted in Figure 1. Under this condition, the *J*-integral is no longer path-independent,[14] and thus the calculation of the crack-tip stress field and the energy analysis of the whole sample will not give the same result. Since the silicate nanolayers and the cooling rate affect both the effective viscosity and the plastic properties, to provide a scientific basis for the optimization of microstructure, the essential work and the nonessential work must be studied separately.

In addition to the global field method and line zone models developed for the numerical simulation of the fracture in polymers,[15–17] there are several experimental techniques that can be used to distinguish the background energy dissipation and the essential work, among which is the technique of double notched sample (DNS).[18,19] As depicted in Figure 2, under the external load the two precracks will grow along the median plane and eventually lead to the final failure. The energy dissipated in the crack tip

*Correspondence to:* Y. Qiao (yqiao@uakron.edu).

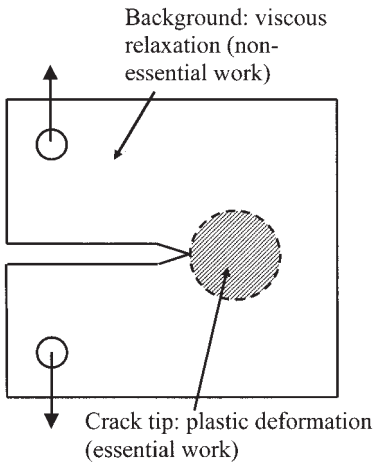


**Figure 1** A schematic diagram of the essential fracture work and the background relaxation.

zone equals the essential fracture work, $W_e$, and the energy dissipated in the background results in the nonessential work, $W_{ne}$, that is:

$$W_f = W_e + W_{ne} \quad (1)$$

When the ligament length, $l$, is larger than about three times the sample thickness, $W_e$ can be assumed proportional to $l$, and $W_{ne} \propto l^2$. Hence, eq. (1) can be rewritten as

$$\bar{W} = \alpha + \beta l \quad (2)$$

where $\bar{W} = W_f/lb$, with $b$ being the sample thickness; $\beta l = W_{ne}/lb$ reflects the nonessential work; $\beta$ is a rate/temperature dependent material parameter; and $\alpha = W_e/lb$ indicates the essential work. By performing a series of tests on samples of different $l$, $\alpha$ can be determined as the extended proportional limit.

In this article, the DNS technique is employed for the measurement of essential fracture work of air cooled and cold water quenched nylon 6-silicate nanocomposites with different silicate contents, through which the combined effects of nonisothermal crystallization and filler-matrix interaction on plastic deformation and viscous relaxation as well as their roles in fracture processes are analyzed.

## EXPERIMENTAL

### Sample preparation

The nylon 6-silicate nanocomposites studied in this article were provided by Dr. M. Kato in the Toyota CRD Lab, Inc. The high degree of exfoliation was achieved through an *in situ* polymerization technique using cation exchanged 12-montmorillonite and ε-caprolactam, followed by mechanical crushing, washing, and drying.[20] Three different materials were tested: N6, NS17, and NS37, with silicate contents of 0 wt %, 1.7 wt %, and 3.7 wt %, respectively.

The as-received material was in pellet form about 2 × 2 × 4 mm large. The pellets were first dried in a type 285A Isotemp vacuum oven at 80°C for 24 h, and then hot pressed into thin films at 240°C using a type 3912 Carver hydraulic compression molding machine. After being kept at this temperature for about 8 min to minimize the influence of the heat treatment history, the thin films were either air cooled with mold or cold water quenched. The mold was made from 304 stainless steel with size around 200 × 200 × 50 mm. The film thickness was about 0.5 mm.

### Fracture experiment

To measure the essential work, tensile experiments were carried out on both air cooled and cold water quenched specimens of N6, NS17, and NS37. Samples with the length of 50.0 mm and the width of 10.0 mm were cut from the hot pressed thin films, and then double notched by using a razor blade. The radius of the notch tip was below 0.1 mm. The ligament length was in the range of 1 mm to about 9 mm. The dimensional requirements discussed by Hashemi[21] for the DNS technique were satisfied.

The fracture tests were performed in a type-5569 tabletop Instron machine at room temperature in displacement control mode. The crosshead speed was 1.0 mm/min. Through the measured load-displacement curves, the total fracture work was calculated as

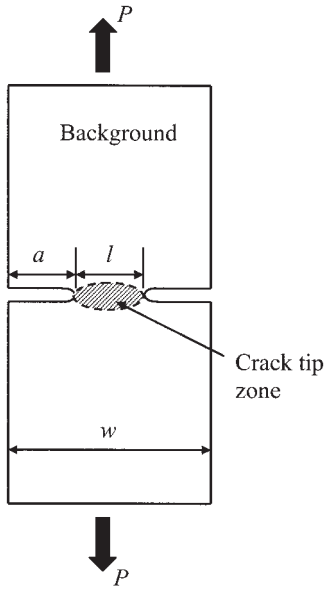


**Figure 2** A schematic diagram of a double notched sample.

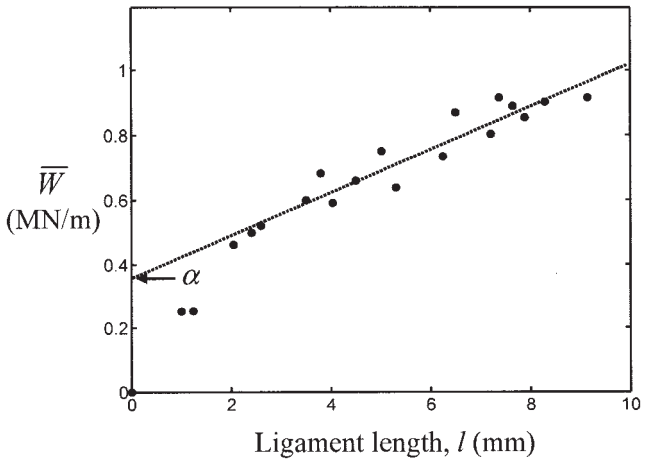


**Figure 3** The experimental data of the $\bar{W}-l$ relation of cold water quenched N6.

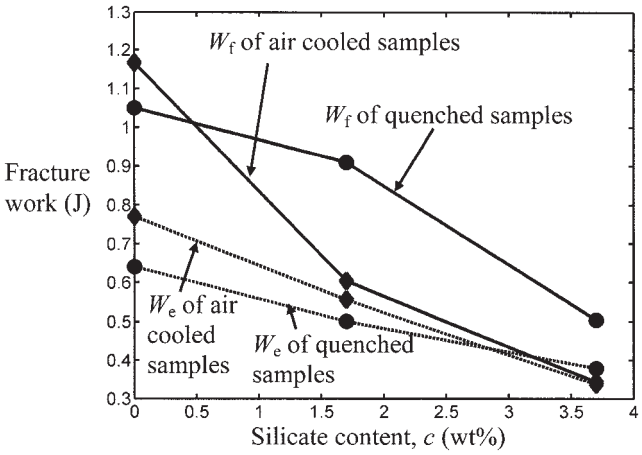


**Figure 4** The experimental results of the total fracture work and the essential fracture work.

$$W_f = \int_0^{\delta_0} P d\delta \quad (3)$$

where $P$ is the applied load, $\delta$ is the displacement, and $\delta_0$ is the ultimate displacement. Figure 3 shows a typical experimental data set of the normalized fracture work, $\bar{W}$ as function of the ligament length, through which the value of $\alpha$ can be determined. The essential fracture work is

$$W_e = \alpha(bl) \quad (4)$$

The results of $\alpha$, $W_f$, and $W_e$ are shown in Table I and Figure 4.

### Loading-unloading experiment

The energy dissipated in the background can be either calculated as the difference between $W_f$ and $W_e$ or directly estimated through the loading-unloading curves of smooth-bar-type samples. Due to the viscous relaxation, during unloading the applied load is considerably lower than that in loading, forming a hysteresis loop. The area of the loop indicates the internal friction.

The specimens were similar with those used in the fracture experiment, except that they were not prenotched. The tests were performed by using the type 5569 Instron machine in displacement control mode. The crosshead first moved up at a constant rate of 1.0 mm/min, and when the set point was reached it returned to the original position at the same speed. Both air cooled and cold water quenched samples were analyzed. The experimental data are shown in Figure 5.

### Wide angle X-ray diffraction scanning (WXDS) analysis

The different fracture resistances of samples of various silicate contents and cooling rates should be attributed to the change in matrix morphology and filler-matrix interaction. Due to the fine semicrystalline structure, the fracture behavior was somewhat similar to that of amorphous materials[22] and was affected by the tie-molecule density, crystallinity, and crystalline structure, which could be analyzed through wide angle X-ray diffraction scanning. The analyses were performed in a 40mA-40kW Bruker AX8 diffractometer with CuK$\alpha_1$ radiation. Details of the sample preparation and scanning process have been discussed elsewhere.[7] The results are shown in Figure 6.

**TABLE I**
**The Essential Fracture Air Cooled and Cold Water Samples**

| | N6 | | NS17 | | NS37 | |
|---|---|---|---|---|---|---|
| | Quenched | Air cooled | Quenched | Air cooled | Quenched | Air cooled |
| Silicate content (wt %) | 0 | 0 | 1.7 | 1.7 | 3.7 | 3.7 |
| $\alpha$ (MN/m) | 0.43 | 0.47 | 0.29 | 0.32 | 0.22 | 0.19 |
| $W_e/W_f$ ($l$ = 3.5 mm) | 0.61 | 0.66 | 0.55 | 0.92 | 0.75 | 0.98 |

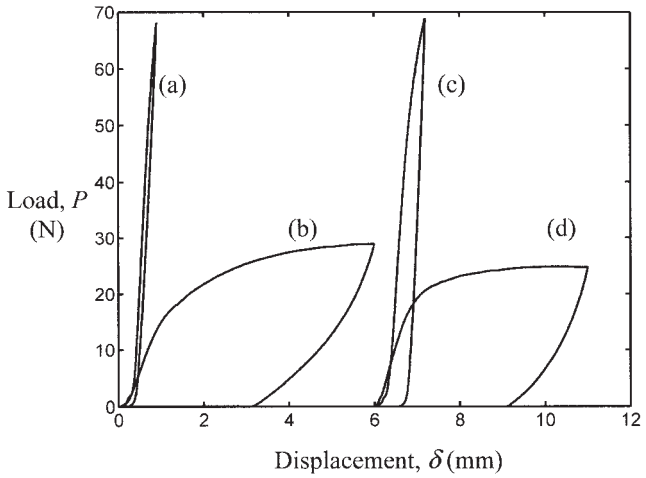


**Figure 5** The hysteresis loops in the load-displacement curves of (a) air cooled N37, (b) air cooled N6, (c) cold water quenched N37, and (d) cold water quenched N6. Note that curves (c) and (d) have been shifted along the horizontal axis.

## DISCUSSION

Through Figure 3 it can be seen that the fracture work increases with ligament length, as it should. Since the essential fracture work is proportional to $l$ while the total fracture work is proportional to $l^2$, the degree of importance of essential work, which can be characterized by the $W_e/W_f$ ratio, keeps decreasing as $l$ rises. When $l$ = 3.5 mm, according to Table I, in both air cooled and cold water quenched samples $W_e/W_f$ is about 60–70%, that is, the amount of energy dissipated in the near-tip field is about twice that of background relaxation. SEM fractography shows that, regardless of the cooling rates, all the fracture surfaces exhibit similar fibrous structures consisting of microvoids and local-drawing zones, indicating that the failure mode in the crack-tip plastic zone is insensitive to the crystallization processes.

In quenched samples, as the silicate content, $c$, increases, the $W_e/W_f$ ratio remains at the same level, ranging from 55 to 75%. In air cooled samples, however, this ratio is increased rapidly to more than 90% when the silicate content exceeds 1.7 wt %, which indicates that the background energy dissipation is negligible due to the presence of the silicate nanolayers. The essential fracture work is affected by the silicate content but is quite insensitive to the cooling rate. As $c$ increases from 0 to 3.7%, the values of $\alpha$ of air cooled and cold water quenched samples decrease by a factor about 2, as shown in Figure 4. When the silicate content is low, the essential work of air cooled samples is somewhat higher, while with the increasing of $c$, the cooling rate effect becomes negligible.

Note that, compatible with the experimental results in single-notched specimens,[7] the total fracture work of double notched nanocomposite samples is a function of cooling rate. In air cooled samples, $W_f$ decreases with increasing $c$, and in cold water quenched samples the values of $W_f$ in NS17 and NS37 are much higher. With relatively low silicate content, the dominant plastic deformation mechanism is cold drawing and is somewhat independent of the isothermal or nonisothermal crystallization processes.[7] Thus, the cooling rate dependence of the total fracture work is quite weak. If the silicate content is high, crazing becomes important. The initiation and growth of crazes are affected by both the matrix morphology and the filler-matrix interaction.[2,3]

In semicrystalline nylon polymers there are two basic crystal forms, $\alpha$ and $\gamma$. The peak reflection angles of $\alpha$ form are at 20.5° and 24°, and that of $\gamma$ form is about 21.5°. As shown in Figure 6, both increasing cooling rate and addition of silicate nanolayers can considerably promote the formation of the $\gamma$ form. The $\gamma$ form is characterized by parallel chains with amide

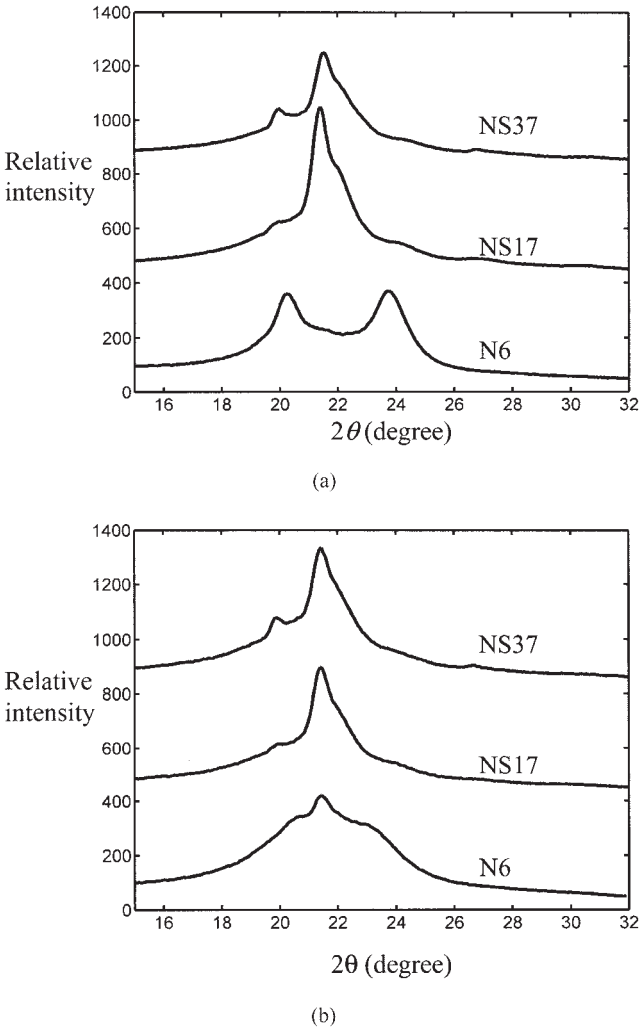


**Figure 6** The WXDS results of (a) air cooled and (b) cold water quenched samples.[7]

groups twisted from methylene group planes, in which, compared with the $\alpha$ form consisting of monoclinic unit cells with a zigzag planar configuration, the chain slippage and relative motion are easier. As a result, the extent of viscous relaxation is higher in the $\gamma$ form and, therefore, the background energy dissipation is more pronounced in cold water quenched samples, even though the crystallinity is about the same.[5–7]

The silicate content and cooling rate dependence of the effective viscosity is also shown in Figure 5. The hysteresis loops in the loading-unloading curves are caused by the relaxation during the quasi-static tests. In cold water quenched samples, again, it can be seen that the degree of relaxation is quite independent of the silicate content. In air cooled samples, with the increasing of $c$, the effective viscosity rises rapidly, and in NS37 the hysteretic behavior is greatly suppressed. Thus, the beneficial effect of increasing the cooling rate to the fracture resistance must be attributed to the change in the viscous properties in the background, instead of the plastic deformation behavior at the crack tip. Note that the nonessential work depends on the sample geometry. As the ligament length becomes larger, the background energy dissipation is increasingly important and the cooling rate effect is more pronounced. In an extreme case, if the prenotch length is zero, that is, in a smooth-bar-type sample, the rupture work dominates the failure process and the essential work is reduced to a negligible level. Once a long crack is formed, the crack growth is determined by the crack-tip plastic deformation, which is insensitive to the crystallization conditions. Consequently, in quenched nanocomposites, the notch brittleness effect is pronounced and prevention of crack initiation or stress/strain concentration is important.

## CONCLUSION

In a previous experimental study,[7] we reported the increase in total fracture work in cold water quenched samples of nylon 6-silicate nanocomposites. In this article, the essential fracture work and the nonessential work were studied separately through the double-notched-sample and loading-unloading experiments. The essential work was related to the crack tip behavior, and the nonessential work was caused by the background relaxation. It was found that the essential fracture work decreased with increasing silicate content, but was somewhat independent of the cooling rate. The nonessential work, on the other hand, was significantly affected by the isothermal or nonisothermal crystallization processes. In cold water quenched samples, the nonessential work was insensitive to the silicate content, while in air cooled samples it decreased rapidly with increasing $c$. Therefore, the factor of cooling rate comes in not by affecting the plastic deformation at the crack tip, but by influencing the effective viscosity of the material in the background. This phenomenon was attributed to the morphology change in the matrix.

We are grateful to Dr. M. Kato in Toyota CRD Lab, Inc., for his help in sample preparation.

## References

1. Kato, M.; Usuki, A. In Polymer-Clay Nanocomposites; Pinnavaia, T. J.; Beall, G. W., Eds.; John Wiley & Sons: New York, 2000; Chapter 6.
2. Yasue, K.; Katahira, S.; Yoshikawa, M.; Fujimoto, K. In Polymer-Clay Nanocomposites; Pinnavaia, T. J.; Beall, G. W., Eds.; John Wiley & Sons: New York, 2000; Chapter 7.
3. Giannelis, E. P. Adv Mater 1996, 8, 29.
4. Masenelli-Varlot, K.; Erynaud, E.; Vigier, G.; Varlet, J. J Polym Sci 2002, B40, 272.
5. Giza, E.; Ito, H.; Kikutani, T.; Okui, N. J Macromolecular Sci-Phys 2000, B39, 545.
6. Tjong, S. C.; Meng, Y. Z.; Xu, Y. J Polym Sci 2002, B40, 2860.
7. Qiao, Y.; Avlar, S. Compos Part A, to appear.
8. Wu, T. M.; Liao, C. S. Macromol Chem Phys 2000, 201, 2820.
9. Liu, X.; Wu, Q. Eur Polym Mater 2002, 38, 1383.
10. Levita, G.; Marchetti, A.; Lazzeri, A. Polym Compos 1989, 10, 344.
11. Chan, C.; Wu, J.; Li, J.; Cheung, Y. Polym 2002, 43, 2981.
12. Labour, T.; Vigier, G.; Seguela, R.; Gauthier, C.; Orange, G.; Bomal, Y. J Polym Sci 2002, B40, 31.
13. Xu, W.; Liang, G.; Wang, W.; Tang, S.; He, P.; Pan, W. P. J Appl Polym Sci 2003, 88, 3093.
14. Hellan, K. Introduction to Fracture Mechanics; McGraw-Hill: London, 1984.
15. Schapery, R. A. Int J Fract Mech 1975, 11, 141.
16. Schapery, R. A. Int J Fract Mech 1975, 11, 369.
17. Schapery, R. A. Int J Fract Mech 1975, 11, 549.
18. Chan, W.; Williams, J. G. Polym 1994, 35, 1666.
19. Wu, J.; Mai, Y. W. Polym Eng Sci 1996, 36, 2275.
20. Usuki, A.; Kojima, Y.; Kawasumi, M.; Okada, A.; Fukushima, Y. J Mater Res 1993, 8, 1179.
21. Hashemi, S. J Mater Sci 1997, 32, 1563.
22. Kambour, R. P. Macromol Rev 1983, 52, 1.